

**Relationship Between Eelgrass Coverage,
Edge Length, and Epifauna Abundance
with UAV Remote sensing: A Case Study
on NorthEast Pacific Coast**

**Tou In Kwan
May 2024**

**Relationship Between Eelgrass Coverage, Edge Length, and Epifauna Abundance
with UAV Remote Sensing: A Case Study on NorthEast Pacific Coast**

A Final Report Presented to
The Faculty of the Department of
Urban and Regional Planning
San José State University

In Partial Fulfillment
of the Requirements for the Degree
Master of Geography

By
Tou In Kwan
May 2024

Acknowledgment

I would like to express my sincere gratitude to all those who have made this project possible and provided extensive biological and drone-collected data for this project:

Bo Yang from San Jose State University, San Jose, CA, USA, Timothy L. Hawthorne from University of Central Florida, Orlando, FL, Lillian Aoki from Cornell University, Ithaca, NY, USA, Deanna S. Beatty from University of California, Davis, CA, USA, Lia K. Domke from University of Alaska Fairbanks, Juneau, AK, USA, Ginny L. Eckert from University of Alaska Fairbanks, Juneau, AK, USA, Carla P. Gomes from Cornell University, Ithaca, NY, USA, Olivia J. Graham from Cornell University, Ithaca, NY, USA, C. Drew Harvell from Cornell University, Ithaca, NY, USA, Kevin A. Hovel from San Diego State University, San Diego, CA, USA, Margot Hessing-Lewis from Hakai Institute, Heriot Bay, BC, Canada, Carmen Ritter from Smithsonian Environmental Research Center, Edgewater, MD, USA, Ryan S. Mueller from Oregon State University, Corvallis, OR, USA, Luba Reshitnyk from Hakai Institute, Heriot Bay, BC, Canada, John J. Stachowicz from University of California, Davis, CA, USA, Fiona Tomas from Instituto Mediterráneo de Estudios Avanzados, CSIC-UIB, Esporles, Spain, and J. Emmett Duffy from Smithsonian Environmental Research Center, Edgewater, MD, USA

I would like to extend my deepest gratitude to my academic advisor, Dr. Bo Yang, for his invaluable support, guidance, and the knowledge he shared along this research journey.

I am also deeply appreciative of Professor Richard Kos' patience, encouragement, and assistance throughout my undergraduate and graduate studies at SJSU.

Table of Content

| | |
|--|----|
| Abstract | 1 |
| Literature Review | 1 |
| Eelgrass & Epifauna Relationship..... | 1 |
| Challenges in Coastal Management and Seagrass Monitoring..... | 4 |
| Advancements in UAV Technology..... | 5 |
| Advancements in Remote Sensing and Image Processing..... | 6 |
| Research Objective | 6 |
| Methodology | 7 |
| Study Sites..... | 7 |
| Data Collection..... | 7 |
| Data Analysis..... | 9 |
| Orthoimagery Generation and Image Segmentation..... | 9 |
| The Calculation of Eelgrass Ratio and Parameter within the Studied Radius..... | 10 |
| Statistical Analyses..... | 12 |
| Result | 14 |
| The Generation of the Orthomosaic Imagery..... | 14 |
| Image Segmentation and Eelgrass Classification Result..... | 15 |
| Digitization Result..... | 16 |
| Buffer Polygons and Further Clean-up..... | 17 |
| The Calculation of Eelgrass Ratio and Eelgrass Edges..... | 19 |
| Linear Regression Result..... | 21 |
| Discussion and Conclusion | 23 |
| Enhanced Eelgrass Habitat Mapping with Drones..... | 23 |
| Eelgrass Coverage/ Edge Length and Epifauna Abundance..... | 24 |
| Temporal Variability of Eelgrass and Epifauna Relationships..... | 24 |
| Limitation and Future Studies..... | 25 |
| Bibliography | 26 |

Abstract

Coastal management in recent years has become more of a challenge due to increasing human disturbance and the lack of inadequacy of a coastal management framework (Adade, et.al., 2021). The widespread use of drone technologies has overcome this obstacle due to their nature of autonomous operations, ease of deployment, and temporal flexibility for catching events like low tides. The cost-effectiveness for both initial deployment and subsequent repeated mapping, combined with their ability to capture detailed information through high-resolution imaging (Yang, et.al, 2022), have made UAVs a potent tool for data collection. This research incorporates the adaptation of UAVs in assessing the conditions of critical eelgrass habitats at several sites along the Pacific Coast. This research aims to encompass the use of drones to provide a more localized and detailed way of analyzing eelgrass, which is a marine flowering plant that is widely recognized for its critical role in supporting and enhancing marine ecosystems, and their habitats. multispectral camera systems mounted on the drone enable researchers to capture high-quality images of the eelgrass to analyze their distribution. In addition, in-situ eelgrass sample collections allow researchers to identify and quantify the population and biodiversity of the epifauna in different eelgrass habitats. Epifauna, including species such as crabs, sea slugs, and various shellfish, are organisms that live on the surface of the seafloor or attach to plants like eelgrass (Whippo, et.al., 2018). Epifauna could be further classified into mobile and sessile groups, with mobile epifauna freely moving about and sessile epifauna remaining fixed in one location (Talyor, 2019). They form a tight food web with eelgrass. Therefore, understanding the distribution of eelgrass meadows and epifauna would be vital for developing strategies for the enhancement of marine biodiversity. This research explores the relationship between eelgrass coverage, edge length, and epifauna abundance from multiple study sites on the Northeast Pacific Coast. The research method demonstrated in

this study provides a more holistic and sustainable framework for coastal management and eelgrass monitoring in the future.

Literature Review

Eelgrass & Epifauna Relationship

Eelgrass (*Zostera marina*) is a marine flowering plant that is widely recognized for its critical role in supporting and enhancing marine ecosystems. It serves as an important habitat for a variety of marine life, including fish and invertebrates. Moreover, seagrass beds are also known for their capability to sequester and store carbon, which plays a crucial role in mitigating the impacts of climate change (Yang, et.al, 2022). Not to mention its ability to regulate ocean pH levels, which alleviates the adverse impacts of ocean acidification (Roman, et.al., 2021). In addition, eelgrass offers shoreline protection by dampening wave energy (Roman, et.al., 2021). It could also prevent coastal erosion with its stabilization of sediments by building up sediments and capturing particles (Ferretto, et.al, 2023). In order to gain a comprehensive understanding of the conditions and function of seagrass ecosystems, an in-depth study of the relationships between eelgrass and epifauna is required

Epifauna are organisms that live on the surface of the seafloor or attach to plants. They form a tight food web with eelgrass. Epiphytes play a critical role in the relationship between eelgrass and epifauna as they are a valuable food source for epifauna that are inhabiting eelgrass meadows (Whippo, et.al., 2018). Epifauna is dependable on epiphytes as it receives the essential nutrients and energy for its survival and growth from them. In addition, other larger marine animals also consume epifaunal species as their food sources, forming a nutrient cycle within the ecosystems (Ferretto, et.al., 2023). Therefore, eelgrass meadows serve as feeding grounds and refuges for a variety of marine organisms, enhancing the overall biodiversity and supporting different ecosystem functions.

Crustaceans and gastropods are some of the most abundant epifauna groups found in the eelgrass habitats. These 2 groups of marine invertebrates play a crucial role in the eelgrass ecosystems (Ward, et.al., 2022). They both belong to the categorization of mobile epifauna due to their ability to move freely (Taylor, 2019). Crustaceans consist of a group of arthropods that rely on eelgrass beds as their shelter and sources of nutrients (Briones-Fourzán, et.al., 2020). Common crustaceans include crabs, shrimps, and lobsters, which belong to the mobile epifauna category. On the other hand, common examples of gastropods include snails and slugs, which are identified by their “head, shells and visceral mass (TRUEMAN, 1983). Previous studies have discovered that the presence of both gastropods and crustaceans is advantageous for eelgrass due to their effectiveness in mitigating the shading effect (Hily, 2004). In the intricate food web of the eelgrass ecosystem consisting of eelgrass, epiphytes, epifauna, and other marine species in the eelgrass ecosystem, an excessiveness of any organisms could pose a threat to the growth of eelgrass. The shading effect occurs when the presence of epiphytic algae or other macroalgae on eelgrass leaves becomes overabundant. This leads to a decrease in light availability due to shading, which adversely affects the photosynthetic activities of the eelgrass (Carman and Gruden, 2018). This phenomenon ultimately diminishes the overall health and the growth rate of eelgrass. However, research has found that certain crab species like *Carcinus maenas* and *Libinia dubia* are beneficial for the growth of eelgrasses thanks to their role as predators of encrusting epiphytes such as sponges (*Demospongiae*) and tunicates (*Ascidacea*) on eelgrass (Carman and Gruden, 2018). Moreover, studies have evaluated the impact of certain gastropods (*Gibbula umbilicalis* and *Jujubinus striatus*) on the grazing of algae biomass and discovered that these gastropods have efficiently reduced epiphytic cover and alleviated the shading effect (Hily, 2004). While both crustaceans and gastropods contribute common benefits to the eelgrass ecosystem, differences in their feeding behaviors and mobility might influence their distribution and abundance within eelgrass meadows. For instance, gastropods typically move more slowly and might have a more limited range of movement compared to crustaceans

(TRUEMAN, 1983). In addition, while crustaceans are omnivores, gastropods are primarily herbivores (TRUEMAN, 1983) (Boström, et.al., 2014).

Despite its significant contributions to marine biodiversity, eelgrass stands as one of the most threatened ecosystems due to various natural, and anthropogenic stressors (Katwijk, et.al., 2015). The decline in the eelgrass population can be traced back to the 19th century (Zoffoli, et.al., 2021). Human-induced disturbances such as industrial and agricultural activities have led to the degradation of water quality (Roman, et.al., 2021). Studies have found that Seagrass wasting disease caused by *Labyrinthula zosterae* has contributed greatly to the loss of eelgrass meadows (Yang, et.al, 2020). With the effects of the warming climate in recent decades, it is observed that the rising sea surface temperature could be detrimental to the eelgrass ecosystems (Graham, et.al.,2023). Eelgrass has an optimal temperature range between 10-25°C and is vulnerable to warm temperatures (Plaisted, et.al., 2022). Ocean temperatures exceeding 25°C could cause significant stress to eelgrass and eventually lead to the death of the plant (Graham, et.al.,2023). With the uncertainties and vulnerabilities that eelgrass is facing, a holistic framework of eelgrass management and conservation is required for protecting the ecosystems and ensuring the long-term sustainability of the marine biodiversity

Challenges in Coastal Management and Seagrass Monitoring

Coastal management has become more of a concern due to increasing human activities and disturbance in the coastal regions. Rapid economic developments result in adverse ecological and environmental impacts on the coastal areas. Shoreline changes have been observed around the globe due to rapid economic growth in coastal cities, where populations and developments tend to concentrate. A study has found that infrastructure projects in the coastal zone near estuaries often bring in hazards such as coastal erosions to the local residents (Tak, et. al, 2020). In addition to the construction of structures, typical commercial activities along beaches also lead to increasing concerns about marine litter found in coastal

dune ecosystems (Andriolo, et.al., 2021). Both studies have discussed how the traditional coastal monitoring framework has been ineffective due to the high equipment and labor costs of conducting coastal surveys (Tak, et. al, 2020). Moreover, the fragile physical conditions of the lands hinder researchers and scientists from assessing the environment without creating unnecessary pollution (Andriolo, et.al., 2021).

Traditionally, seagrass monitoring approaches revolve around the use of airborne or satellite remote sensing techniques at a broader scale across different regions, and the smaller scale method of in-situ field survey to take a closer look at the conditions and stressors of the seagrass leaves (Duffy, et.al., 2019). While these measures have been successful in tracking the status of seagrass and detecting the change of distribution over time, there are limitations associated with them. Observations in aerial or satellite imagery only allow the view and identification of seagrass at a relatively shallow depth due to their low resolution. (Duffy, et.al., 2019). Publicly obtainable satellite imagery such as the Landsat dataset only offers data with a relatively low spatial resolution of 30 m (Tahara, et.al., 2022). Although previous studies have demonstrated that imagery from commercial satellites such as RapidEye, PlanetScope, and Quickbird provides more promising results of seagrass delineation due to their high-resolution imagery, the associated cost with the imagery is deemed unsustainable for long-term seagrass monitoring programs (Coffer, et.al. 2020).

Advancements in UAV Technology

The utilization of Unmanned Aerial Vehicles (UAVs) in assessing the condition of sensitive habitats has become more prevalent in recent decades. The advancement in UAV technologies has enabled individuals and researchers to conduct studies more accurately and efficiently. A study introduced the various types of unmanned aircraft and their advantages in providing a safe method of collecting data in remote and inaccessible regions (Klemas, 2015). It discussed how quadcopter UAVs have become one of the most desirable tools in environmental mapping and habitat monitoring. In addition to their inexpensive costs, quadcopter drones also

offer excellent maneuverability. The ease of deployment of drones allows researchers to operate the drones freely over the study sites without endangering the susceptible physical condition of the lands (Colomina and Molina, 2014). While drone operations are still vulnerable to environmental factors like cloud cover and wind speed that are uncontrollable, the flexibility to schedule a deployment is still a huge improvement over the limitations of geostationary orbit satellites (Tahara, et., 2022). Many of the drones equipped with integrated camera systems on the market cost even less than \$1000 (Klemas, 2015). With the advantages and reliabilities that drones have, a study has found that they could be deployed on a wide range of missions, including emergency responses, disaster management and assessment, habitat and ecological mapping, and urban planning and development (Kandro, et.al, 2021). The use of drones has also demonstrated effectiveness in identifying and assessing eelgrass habitats (Favaro and Zargarpour, 2017). With the correct adjustment of altitude, overlap, and direction of flight, the extent of eelgrass beds could be visualized using drones.

Advancements in Remote Sensing and Image Processing

The function of autonomous mapping combined with the integrated camera systems on drones enables high-resolution images to be captured in real-time during the mapping mission. Captured images would be temporarily stored in an SD card and subsequently be processed by software designated for drone image processing, such as ArcGIS Drone2Map (Yang, et.al, 2019). An orthomosaic and a Digital Surface Model (DSM) are the main products generated from the abovementioned software. The photogrammetry technique in drone cameras and software plays a critical feature in reconstructing the ground surface; while the image stitching approach combines hundreds of drone images and creates a high-quality result imagery of the mapping area (Colomina and Molina, 2014). Furthermore, various features in the orthomosaic can be identified and classified using spatial processing tools such as ArcGIS Pro and Trimble eCognition that contain a variety of pixel-oriented or object-oriented supervised classification methods (Andriolo, et.al., 2021). In recent years, more studies have utilized deep learning

techniques in classifying imageries due to their high accuracy compared to conventional classification methods (Tahara, et., 2022).

Research Objective

In this study, we aim to investigate 2 primary research objectives regarding the relationship between eelgrass coverage, along with edge length, and epifauna abundance. Our first objective seeks to determine whether a higher percentage of eelgrass correlates with increased epifauna abundance. Secondly, we explore the hypothesis of whether a longer eelgrass edge provides greater accessibility to epifauna, potentially resulting in a higher epifauna abundance. Concerning the type of epifauna in our study, we primarily focus on Gastropods and Crustacea due to their different feeding behaviors and mobility. These 2 creatures often use eelgrass not only as a food source but also as a nursery and shelter (Hily, 2004). Contrasting the abundance of these 2 organisms would provide insights into how the distribution of eelgrass would influence their habitat preference.

Despite the intricacies of the relationship between eelgrass and epifauna have previously been investigated by other researchers (Ferretto, et.al, 2023), fewer adapted UAV remote sensing as part of the data collection and research method. By flying at lower altitudes, UAV mapping could achieve a 1.5 cm resolution, enabling a more precise examination of eelgrass structure and distribution from the orthomosaic imagery (Yang, et.al, 2023). This research aims to encompass the use of drones to provide a more localized and detailed way of analyzing eelgrass habitats.

Methodology

Study Sites

It is well acknowledged that Unmanned aerial vehicles (UAV) technologies have been proven to be a prominent and effective way of assessing ecosystems that are sensitive to human intervention, due to their capabilities, endurance, and ranges (Adade, et.al., 2021).

Therefore, the data collection framework of this study revolves around the use of drones as the primary tool in capturing high-resolution imagery of seagrass meadows at the study sites. The nature of this research is primarily quantitative-oriented. This research consists of 27 study sites along the west coast of the US and Canada, as displayed in Table 1. Figure 1 illustrates the map of the study sites, as well as images captured on-site from each region. These coastal areas have been habitats for numerous marine organisms. However, the prevalent wasting disease observed in seagrass meadows has led to the drastic decline of eelgrass populations in recent years (Yang, et.al, 2022). As previous studies have examined the benefits provided by seagrass to the surrounding coastal communities (Ferretto, et.al, 2023), the decrease in eelgrass quantity could potentially cause adverse impacts on the ecosystems as a whole.

Data Collection

A number of drone images were captured during the flight missions at the study sites from 2019 to 2022 using a model DJI Phantom 4 Pro drone which was equipped with an RGB camera sensor (12.4m pixels) (Yang, et.al, 2022). Data was collected primarily during the Summer months (June - July). To ensure a clearer and more observable assessment of the eelgrass distribution, the flight missions were conducted during the morning hours, taking advantage of the low tides. The flight mission was pre-defined in advance and set to cover a subset of the coastline. A 75% overlap was set for both front and side overlaps for easier image processing and stitching subsequently (Yang, et.al, 2022). In addition, the flight attitude was ~60m and the flight for each site lasted about 30 minutes. Figure 2 shows drone piloting on-site capturing images of the eelgrass

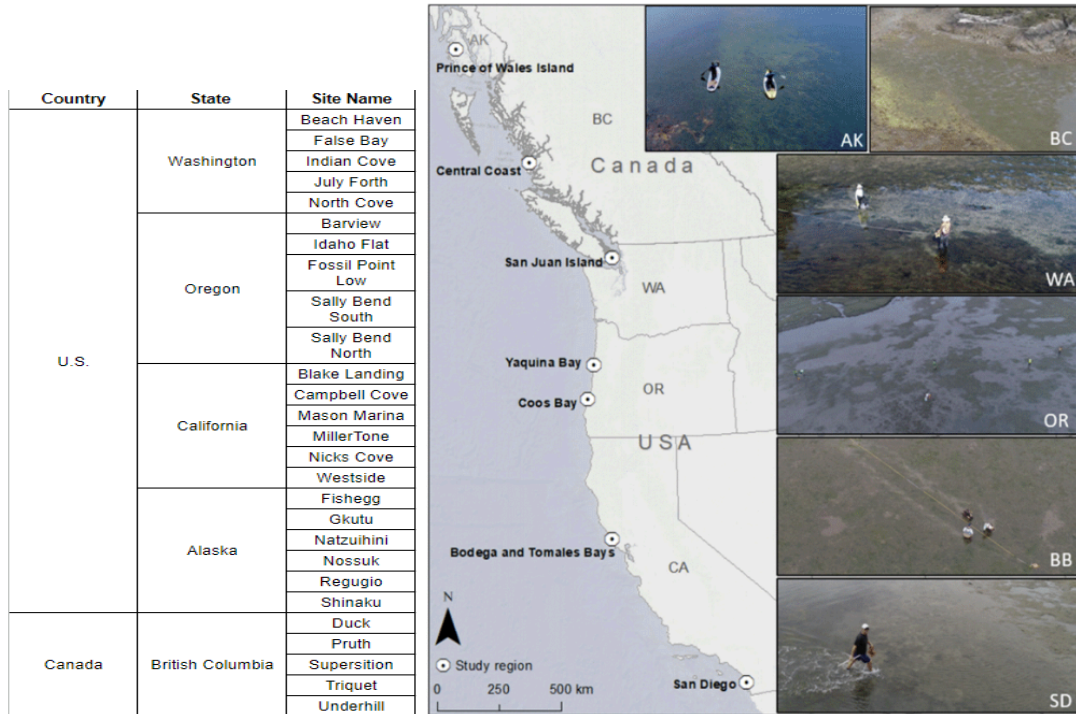


Table 1 & Figure 1. A list of all 27 study sites along the west coast of the US and Canada, as well as a map illustrating the location of the study sites in different regions (Yang, et.al, 2022).

In addition to imagery data captured from the drone, in-situ data collection was conducted on the scene in the meantime. Our partner team on the biological aspects established a total of 6 transects along the coastline at each site, as part of the biological data sampling procedures. Each transect line covered a length of 20m, and epifauna data was gathered at 2 points along the transect tape (at 4m and 16m from the starting point). Individual sample points were assigned unique codes for easier differentiation to facilitate later data analysis. It was ensured that the drone's flight path adequately covered the area where the transect tapes were. The sample collection method involved affixing a container to a pole to capture and collect epifauna from the water, as displayed in Figure 3. Subsequently, the collected samples were taken to the lab for further processing- epifauna species were extracted and identified and abundance was quantified



Figure 2. Drone piloting on-site capturing photos of the eelgrasses.



Figure 3. On-site epifauna data collection.

Data Analysis

Orthoimagery Generation and Image Segmentation

The captured drone images were first processed and stitched together using ArcGIS Drone2Map. ArcGIS Drone2Map is known for utilizing the SfM-MVS photogrammetric technology to align and merge multiple overlapping images (Yang, et.al, 2019). Output from the program generally consists of different 2D and 3D products. An orthomosaic image was the primary output that was utilized for the subsequent analyses.

The generated result would then be segmented using Trimble eCognition. The software was utilized to break up the image into numerous smaller areas through the multiresolution segmentation algorithm, an image segmentation technique. Following the parameter defined in the previous study, the scale parameter was set to be in a range of 20 to 60, along with a 0.2 shape and 0.5 compactness parameter (Yang, et.al, 2022). The objective of this process is to extract areas with the presence of eelgrass from the imagery. Therefore, the supervised classification method from the program would allow users to train and select a number of sampled zones. 2 classes were specified: Eelgrass and Others. A screening was then performed to manually select a few training areas for each class. Then, a classification analysis was run to assign each segmented area a new class. Figure 4 displays the interface of the

software. The program utilized object-orientated classification, which is a technique that groups a set of pixels into meaningful objects according to their spectral characteristics; while the traditional pixel-based classification method takes into account the individual pixels independently (Yang, et.al, 2019). The above-mentioned shape, scale, and compactness parameters are all part of the spectral properties that would influence the result of the segmentation. The shape parameter controls the sensitivity of the object shape; the compactness parameter determines the smoothness of the object boundaries; and the scale parameter influences the size of the smallest objects that will be segmented (Andriolo, et.al., 2021). The results generated from the image segmentation process will then be exported to ArcGIS Pro to conduct further analysis

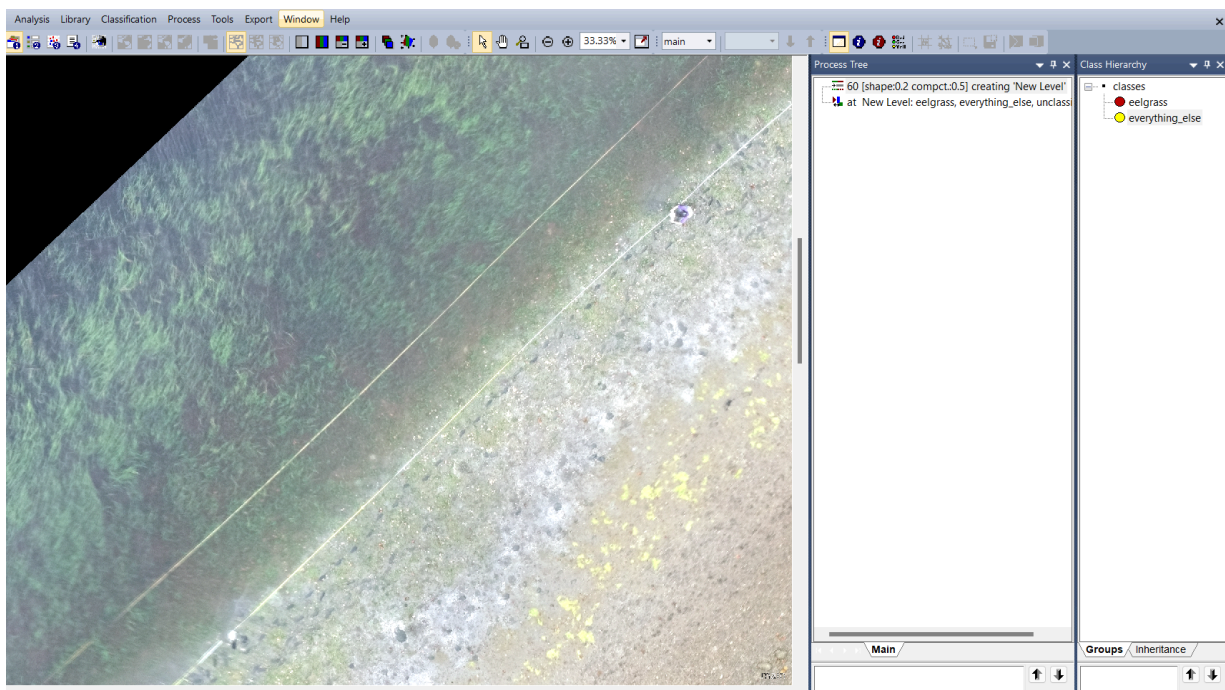


Figure 4. Interface of Trimble eCognition. The image in the center would be segmented as part of the analysis, while the sections on the left display the pending multiresolution segmentation algorithm and the specified classes.

The Calculation of Eelgrass Ratio and Parameter within the Studied Radius

The next step of the research analysis encompassed the utilization of ArcGIS Pro. The study defined several studied radii around the sampling points. We decided to focus on investigating the extent of seagrass coverage within a radius of 2 meters, 1 meter, and 0.5 meters, respectively. The choice of the radius was based on the varying active ranges and mobilities of the epifauna; certain marine species are capable of swimming longer distances, while others are constrained to a specific size range. While the 0.5-meter zone is used to observe species with less mobility, the larger 1 and 2-meter radii are intended to capture the activity of more mobile species that utilize larger areas for feeding and shelter. The various buffer sizes offer a comprehensive view of how eelgrass morphology, patch sizes, and shapes influence the accessibility and distribution of epifauna species. The analysis began with the digitization of the transect lines that were visible from the drone orthomosaic. Utilizing the “Create Points Along Lines” tool to create 2 points per transect line, as shown in Figure 5, a total of 12 points were digitized per study site per year. The 2 points referred to the locations where the epifauna data was collected during the in-situ sample collection, which are at 4m and 16m from the starting point.

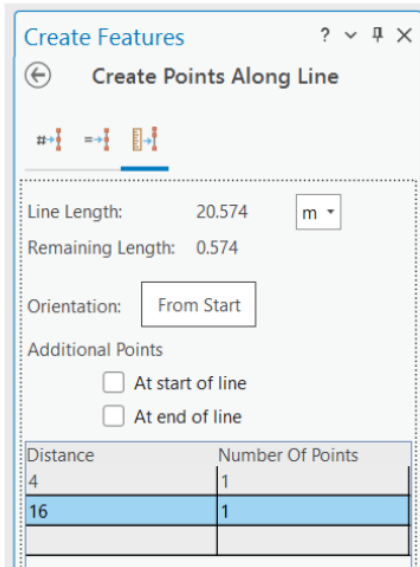


Figure 5. ArcGIS Pro interface of the editing tool Create Points Along Line used to digitize the 4 and 16-meter sampled points.

The framework of the study is to figure out the ratio of eelgrass within a given radius, along with the parameter of the eelgrass. Therefore, after the creation of buffer zones for the individual sampling points, the “Intersection” tool was run to investigate the area of eelgrass that overlapped with the buffer zones. The objective of the analysis was to delineate the eelgrass region, which was extracted in the previous step of image segmentation, using defined buffer zones. Since the eelgrass areas remained in small fragmented segments that were broken up from the segmentation process, the “Dissolve” tool was subsequently applied to merge the individual polygons of eelgrass within each buffer zone into a single unit. Figure 6 provides a snapshot of the ArcGIS Pro interfaces of the tools used in this process

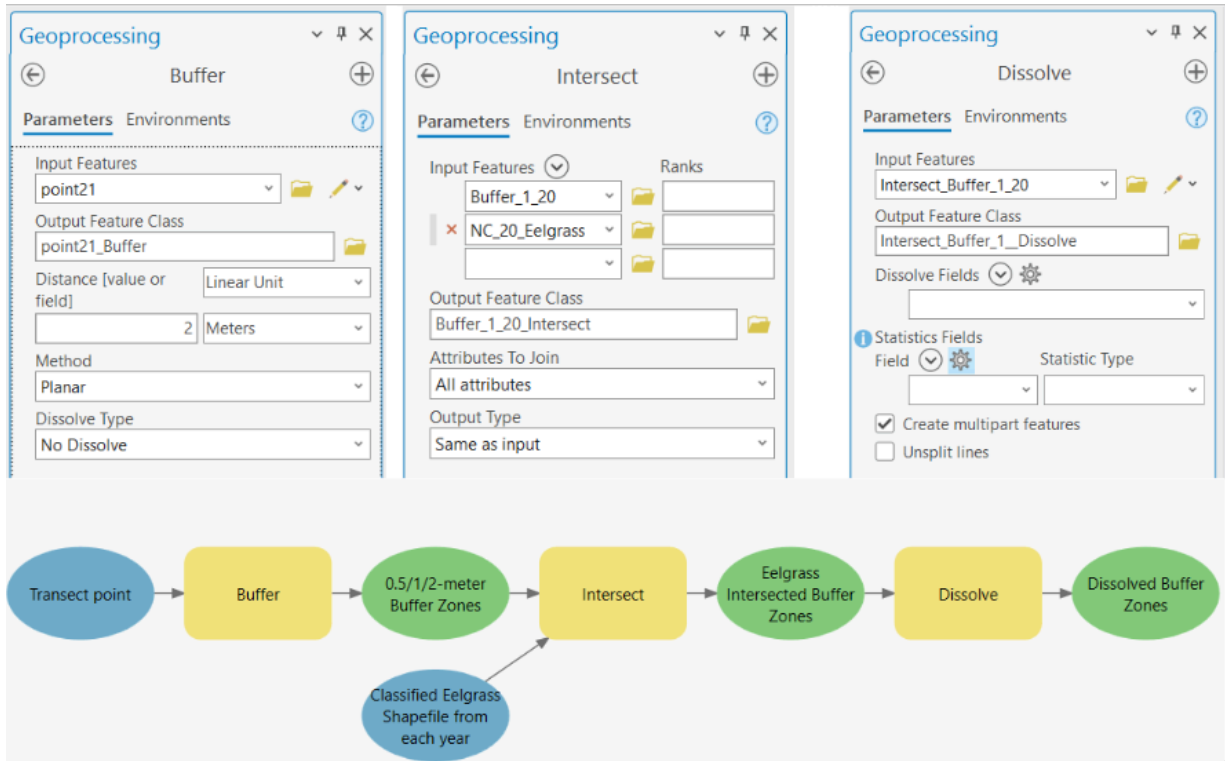


Figure 6. ArcGIS Pro interfaces of the geoprocessing tools Buffer, Intersect, and Dissolve. The section below illustrates the workflow from ArcGIS Model Builder.

To automate and expedite the process, analyses were conducted with a series of Python codes run in ArcGIS Pro Python Window. Figure 7 indicates a Python script that was run for the 2-meter study radius. The iteration was executed for the 1-meter and 0.5-meter radius subsequently. Last but not least, the automation from the Python codes would print out the “Area” and “Perimeter”, which are attributions stored within the Dissolve output feature class, of each eelgrass buffer zone in the Python window. The 2 values would help address the research question regarding the eelgrass percentage and edges.

Python

```
import arcpy

# Set the workspace and environment settings
arcpy.env.workspace = r"D:\geog\282\FinalProject\Northcove\NorthCove\NorthCove.gdb"
arcpy.env.overwriteOutput = True

# Input files
point_fc = "point19"
seagrass_fc = "NC_19_Eelgrass_New"

# Buffer distances
buffer_distances = [2.0, 1.0, 0.5] # Use numeric values for buffer distances

# List to store dissolved polygon feature classes
dissolved_fc_list = []

# Step 1: Create buffer zones and convert to Line feature class
for buffer_distance in buffer_distances:
    buffer_fc_list = []

    with arcpy.da.SearchCursor(point_fc, ["OID@", "SHAPE@"]) as cursor:
        for row in cursor:
            output_buffer_fc = "Buffer_" + str(row[0]) + "_" + str(buffer_distance).replace(".", "") # Remove decimal point
            arcpy.Buffer_analysis(row[1], output_buffer_fc, str(buffer_distance) + " Meters")
            buffer_fc_list.append(output_buffer_fc)

            # Convert the buffer polygon feature class to Line feature class
            output_line_fc = "BufferLine_" + str(row[0]) + "_" + str(buffer_distance).replace(".", "") # Remove decimal point
            arcpy.FeatureToLine_management(output_buffer_fc, output_line_fc)
            buffer_fc_list.append(output_line_fc)

# Step 2: Intersect the buffer lines with the seagrass shapefile
intersect_fc_list = []

for buffer_line_fc in buffer_fc_list:
    output_intersect_fc = "Intersect_" + buffer_line_fc
    arcpy.Intersect_analysis([seagrass_fc, buffer_line_fc], output_intersect_fc)
    intersect_fc_list.append(output_intersect_fc)

# Step 3: Dissolve the intersection results
for intersect_fc in intersect_fc_list:
    output_dissolve_fc = "Dissolve_" + intersect_fc
    arcpy.Dissolve_management(intersect_fc, output_dissolve_fc)
    dissolved_fc_list.append(output_dissolve_fc)

# Iterate through dissolved feature classes and print the "Shape_Length" values
for fc in dissolved_fc_list:
    with arcpy.da.SearchCursor(fc, ["SHAPE@", "Shape_Length"]) as cursor:
        for row in cursor:
            print("Layer:", fc)
            print("Shape_Length:", row[1], "meters")
            print("-" * 40)
```

Figure 7. Python script used to execute the “Buffer”, “Intersection”, and “Dissolve” tools all at once.

Statistical Analyses

After the data of the eelgrass area and perimeter were gathered, the inputs from all the study sites were consolidated with the corresponding epifauna abundance data to conduct a linear regression test. The statistical analysis aimed to investigate the relationship between eelgrass percentage coverage (ratio) and edge length and epifauna abundance. Gastropod and crustacean abundance was a primary focus of the study. Utilizing a linear regression test would help examine how different eelgrass coverage and edge length would influence the abundance

of epifauna species within the buffer zones of various distances from the eelgrass at the sampled transect points.

The linear regression model was designed with the eelgrass coverage and ratio as the independent variables and the epifauna/ gastropod/ crustacean abundance as the independent variables. The study was divided into 2 sets. In the first set of the analysis, data collected from all years would be used to conduct multiple regression tests. For each buffer size of the eelgrass converge and edge length, 3 separated regression tests were performed: 1 focusing on eelgrass and epifauna abundance, 1 analyzing eelgrass and gastropod abundance, and 1 targeting eelgrass and crustacean abundance. Given that these analyses were conducted across different buffer sizes (0.5, 1, and 2 meters), this methodology resulted in a total of 18 distinct regression tests. In the second set of the regression analysis, temporal variations were incorporated as a factor into the model. We focused on data from the years of 2019 and 2021 specifically. Similar to the first set of analyses, the process would also examine the correlations between the eelgrass ratio/edge and the biological variables of epifaunas. By focusing on the data from specific years, we hoped to investigate whether epifauna abundance was influenced by the distribution of eelgrass habitats over time. The second part of the analysis resulted in 36 individual regression tests. Figure 8 displays the process diagram summarizing the steps of the research methodology

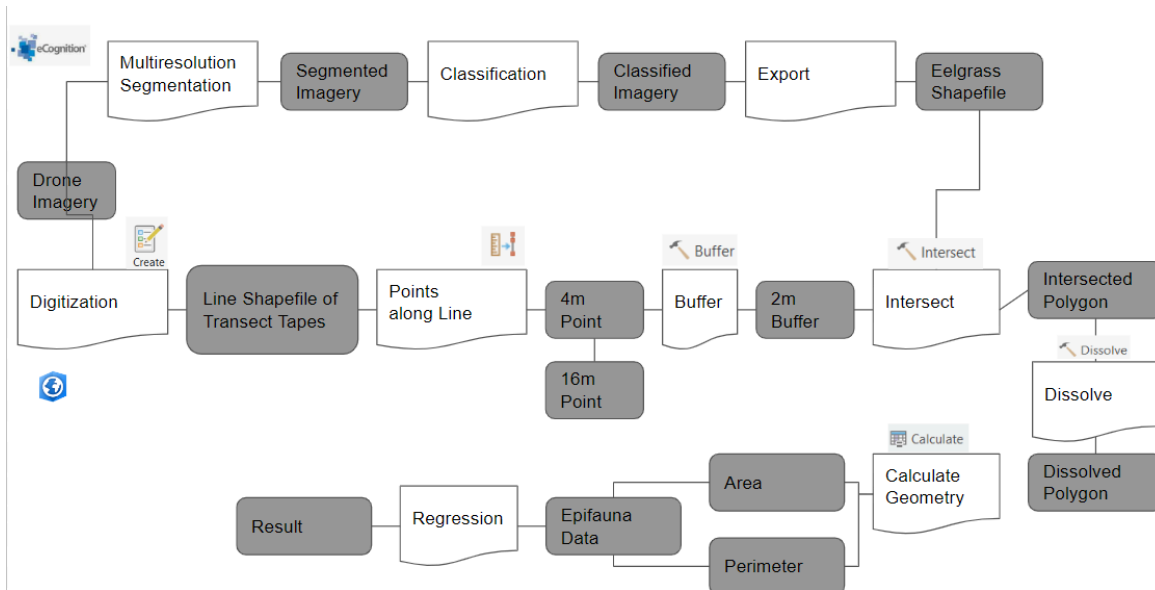


Figure 8. Process diagram summarizing the data analysis sections- including process from both Trimble eCognition (upper section) and ArcGIS Pro (lower section).

Result

The Generation of the Orthomosaic Imagery

A total of 92 orthomosaics were collected and processed as the products of the drone image stitching process. The imageries were exported in TIFF format for subsequent processing in ArcGIS Pro. Imageries were then clipped to smaller areas surrounding the deployed transect tapes. This approach was taken since our samples were collected exclusively along these transects and it would be essential to focus our analysis on these specific areas. The new boundaries of the clipped imageries were ensured at least a 20 m distance away from the transect tape, allowing enough space for the creation of buffer zones and further analysis. Examples of these pre and post-clipped orthomosaics are provided in Figures 9 and 10



Figure 9. The 2D orthomosaic generated from ArcGIS Drone2Map for the 5 Washington sites.

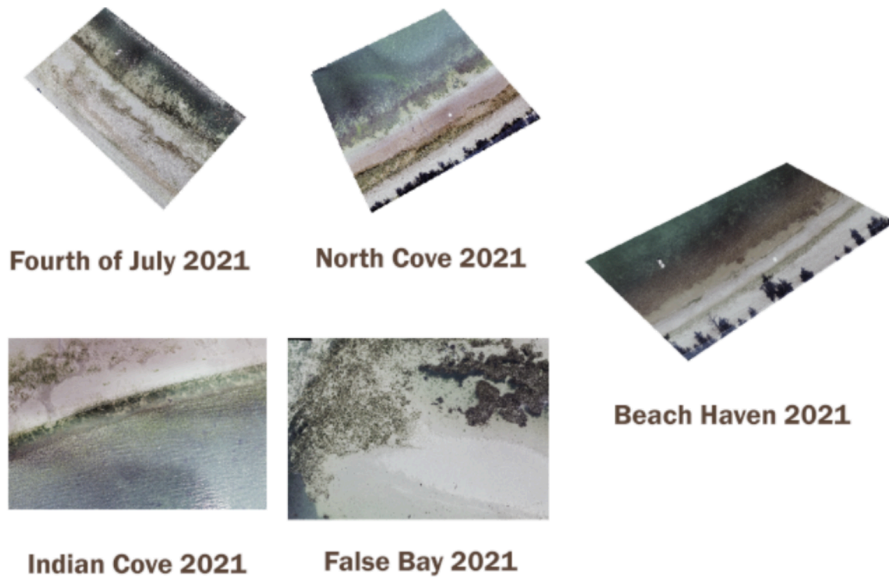


Figure 10. Orthomosaics clipped to the study area surrounding the transect tapes. Washington 2021.

Image Segmentation and Eelgrass Classification Result

Figure 11 illustrates the result of the multi-resolution segmentation from eCognition for the 2021 Beach Haven orthoimage (left image). The input clipped imagery was split into smaller polygons in accordance with the parameters pre-defined. Upon discrete examination of the

imagery, designated segments that contained eelgrass area would be selected as training data. As the research focused solely on the area of eelgrass, other land cover types would belong to the “Other” category when training the samples. As a result, the right image displays the output of the classification process, with red-outlined polygons representing the eelgrass zones and yellow-outlined polygons representing features other than eelgrass.

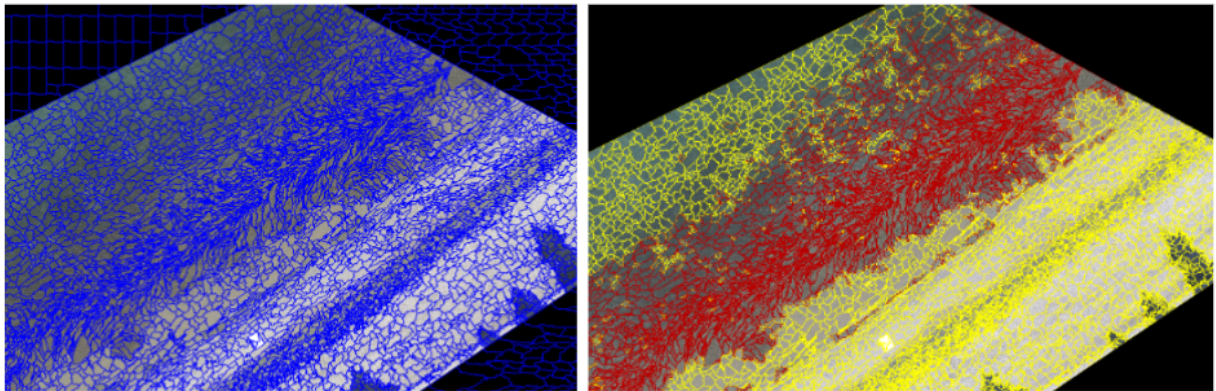


Figure 11. Result of multi-resolution segmentation (left) and classification (right) process for 2021 Beach Haven clipped orthomosaic.

Digitization Result

The classified eelgrass areas exported as a shapefile from eCognition were added into ArcGIS Pro for subsequent analyses. The before (left) images depicted in Figure 12 display the unprocessed clipped imagery along with the digitized transect tapes (as Line feature classes) and the 4 and 16-meter sampled points (as point feature classes); while the after (right) images showcase the addition of the exported eelgrass results, delineated in colored polygons, for the 2 example sites in Washington. The classification result accurately distinguished eelgrass from surrounding features such as sands, rocks, algae, and water based on the selected training data areas.

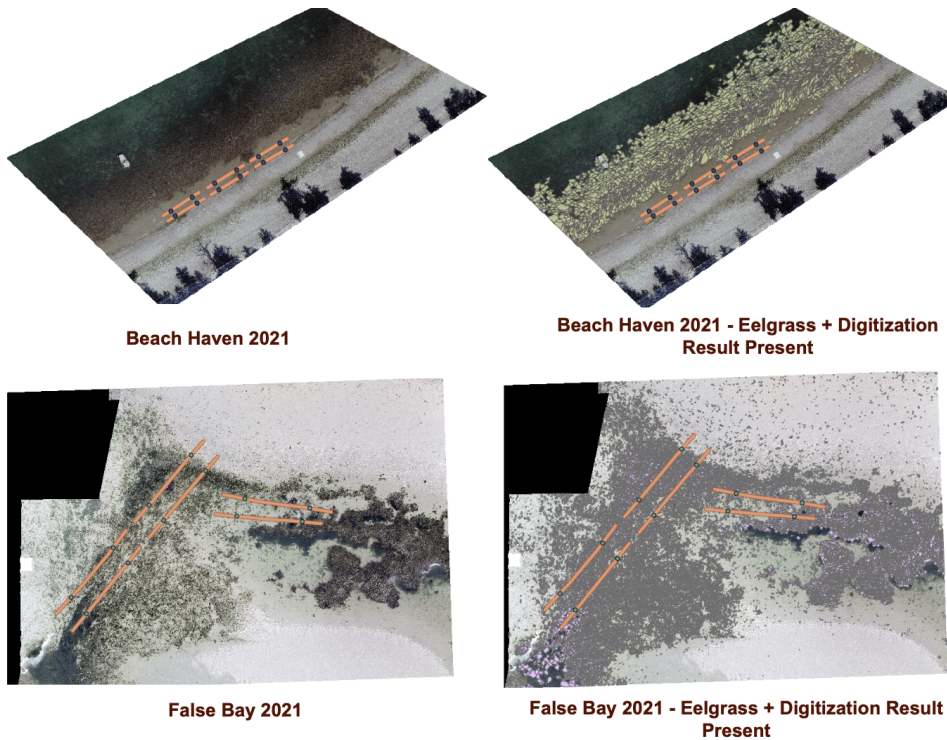


Figure 12. Comparisons of pre and post-processing images. Left: Clipped orthomosaic alongside the digitized transect tapes and sampled points for Beach Haven and False Bay 2021. Right: Clipped orthomosaic with the addition of Eelgrass polygon shapefile (colored polygons) alongside the digitized transect tapes and sampled points for Beach Haven and False Bay 2021.

Buffer Polygons and Further Clean-up

The geoprocessing tools “Buffer”, “Intersect”, and “Dissolve” were successfully executed in ArcGIS Pro with the Python script referenced earlier for all sampled points. Figure 13 showcases the results of a specific study site, Millerton, CA. In addition to the overarching result presented on the left, the images on the right depict a close-up view of how the respective buffer zones interact with the eelgrass areas, as the outcome of the “Intersect” and “Dissolve” tools.



Figure 13. Left: The result of the buffer zone generations on the sampled points and the outcome of the “Intersect” and “Dissolve tools” alongside the digitized transect lines and sampled points. Right: Close-up view of the intersection between the buffer polygons and the eelgrass areas at 2, 1, and 0.5-meter radius.

However, an issue was identified in the eelgrass classification results. Despite being actual eelgrass locations, some areas where transect tapes overlaying the eelgrass were not considered during the classification process as they were not selected as part of the training data. In order to address this issue and improve the accuracy of the analysis, especially the perimeter, manual examinations and digitizations were conducted to include these areas within the intersected buffer zones. The digitization process primarily utilized the “Trace Along” function from ArcGIS Pro’s Editing Tools to redraw eelgrass along the outline of the transect tapes. Figure 14 illustrates the pre and post-digitization results of the process. The left (before) image displays the unprocessed eelgrass buffer zones, where eelgrass appears carved out due to the absence of classification at the transect tapes; while the images on the right showcase

the digitization result, where eelgrass was redrawn over the transect tape areas after detailed examination.

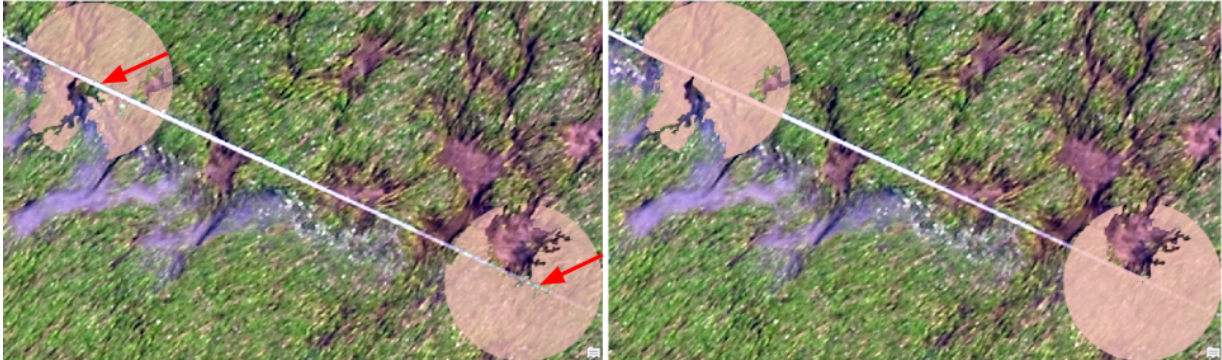


Figure 14. Comparison of the pre and post-digitization of the eelgrass polygons on transect tape area for one of the sampled buffer zones in Millerton, CA. The left image displays the pre-digitization state of the eelgrass polygons, where eelgrass underneath transect tapes was excluded from the classification process; the right image illustrates the post-digitization result, where eelgrass polygons were digitized over the transect tape areas.

The Calculation of Eelgrass Ratio and Eelgrass Edges

The 2 metrics, “Area” and “Perimeter”, played a key role in assessing eelgrass distribution and epifauna abundance. Utilizing the Python script mentioned earlier, these metrics could be generated relatively swiftly. However, we discovered a discrepancy in our approach to calculate the eelgrass edges (perimeter). Taking the 2-meter intersected buffer zone as an example, Figure 15a displays the eelgrass outline that was considered as the “Perimeter” in the initial geoprocessing approach. Yet, as shown in Figure 15b, the incorrect and over-included yellow outline resulting from the “Intersect” tool represents the buffer zone outline rather than the actual eelgrass edges. In fact, the outline highlighted in purple in Figure 15c illustrates the true eelgrass edges that should have been extracted.

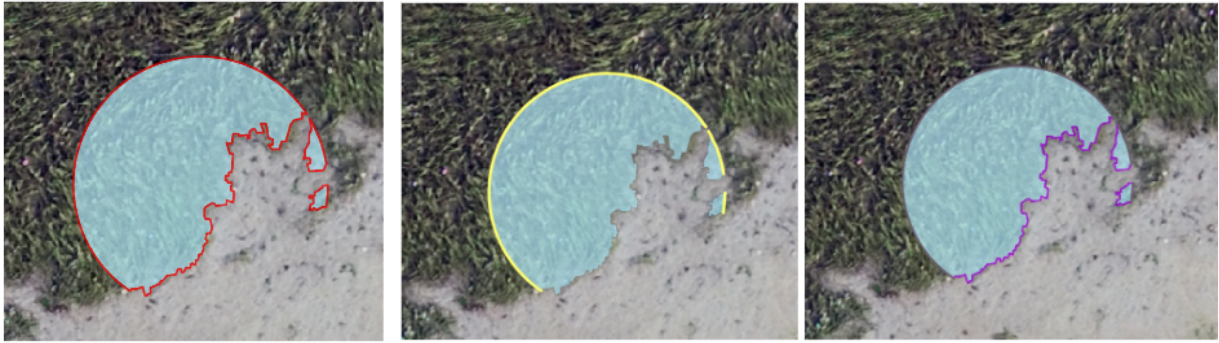


Figure 12a

Figure 12b

Figure 12c

Figure 15. Comparison of buffer zone outline and the actual eelgrass edges from study site Beach Haven, Washington. Figure 15a illustrates the outline (red) of the intersected buffer zone and eelgrass polygons; Figure 15b displays the outline (yellow) of the intersected buffer polygon only, which was intended to be excluded; Figure 15c indicates the outline (purple) of the actual eelgrass perimeter, which would be the final result.

Therefore, our process was refined to specifically isolate and exclude the buffer zone outlines from the calculation of the eelgrass edges. After generating the buffer polygons, the geoprocessing tool “Polygon to Line” was used to extract their boundaries, as displayed in Figure 16). These boundary line feature classes were then intersected with the eelgrass polygons, similar to the approach taken for the buffer polygons. Subsequently, the outlines were further dissolved, and the result (Figure 12b) was subtracted from the original eelgrass perimeter (Figure 15a). The supplementary steps would result in the output illustrated in Figure 15c. Figure 17 depicts a revised Python script showcasing the additional geoprocessing tools that were utilized.

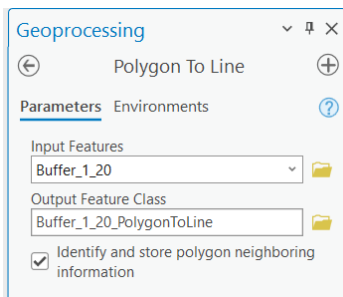


Figure 16. ArcGIS Pro interface of the geoprocessing tool Polygon to Line used to convert the Buffer polygons to Buffer lines

Python

```
import arcpy

# Set the workspace and environment settings
arcpy.env.workspace = r'D:\geog\282\FinalProject\Northcove\NorthCove\NorthCove.gdb'
arcpy.env.overwriteOutput = True

# Input files
point_fc = "point19"
seagrass_fc = "NC_19_Eelgrass_New"

# Buffer distances
buffer_distances = [2.0, 1.0, 0.5] # Use numeric values for buffer distances

# List to store dissolved polygon feature classes
dissolved_fc_list = []

# Step 1: Create buffer zones and convert to Line feature class
for buffer_distance in buffer_distances:
    buffer_fc_list = []

    with arcpy.da.SearchCursor(point_fc, ["OID@", "SHAPE@"]) as cursor:
        for row in cursor:
            output_buffer_fc = "Buffer_" + str(row[0]) + "_" + str(buffer_distance).replace(".", "") # Remove decimal point
            arcpy.Buffer_analysis(row[1], output_buffer_fc, str(buffer_distance) + " Meters")
            buffer_fc_list.append(output_buffer_fc)

            # Convert the buffer polygon feature class to Line feature class
            output_line_fc = "BufferLine_" + str(row[0]) + "_" + str(buffer_distance).replace(".", "") # Remove decimal point
            arcpy.FeatureToLine_management(output_buffer_fc, output_line_fc)
            buffer_fc_list.append(output_line_fc)

# Step 2: Intersect the buffer lines with the seagrass shapefile
intersect_fc_list = []

for buffer_line_fc in buffer_fc_list:
    output_intersect_fc = "Intersect_" + buffer_line_fc
    arcpy.Intersect_analysis([seagrass_fc, buffer_line_fc], output_intersect_fc)
    intersect_fc_list.append(output_intersect_fc)

# Step 3: Dissolve the intersection results
for intersect_fc in intersect_fc_list:
    output_dissolve_fc = "Dissolve_" + intersect_fc
    arcpy.Dissolve_management(intersect_fc, output_dissolve_fc)
    dissolved_fc_list.append(output_dissolve_fc)

# Clean up buffer and intersection feature classes
arcpy.Delete_management(";".join(buffer_fc_list + intersect_fc_list))

# Iterate through dissolved feature classes and print the "Shape_Length" values
for fc in dissolved_fc_list:
    with arcpy.da.SearchCursor(fc, ["SHAPE@", "Shape_Length"]) as cursor:
        for row in cursor:
            print("Layer:", fc)
            print("Shape_Length:", row[1], "meters")
            print("-" * 40)
```

Figure 17. Revised Python script used to execute this process refinement

Linear Regression Result

To reinstate the statistical analysis process, 2 sets of linear regression tests were performed to assess the potential correlation between eelgrass coverage/edge length and the abundance of various epifauna species. The analyses looked into several buffer sizes across different years. While the first set of regression tests investigated combined data from all years, the second set evaluated data from 2019 and 2021 separately.

Table 2 below displays the results of the first set of analyses. Despite the fact that the results for the 0.5 m and 1 m buffer zones from the eelgrass coverage side did not achieve any statistical significance at $p\text{-value} \leq 0.1$, it was observed that the 2 m buffer zone showed an

exception with the p-value from the regression test between eelgrass coverage and gastropod and crustacean abundance being ≤ 0.1 . Specifically, the correlation between eelgrass coverage (ratio) and gastropod abundance from the 2 m buffer results showed a p-value of 0.042741. Similarly, the relationship between eelgrass coverage and crustacean abundance indicated a p-value of 0.067126. These results suggested a potentially significant interaction between eelgrass coverage and gastropod and crustacean abundance. However, it was noticed that the R-squared value from both results was relatively low, with eelgrass coverage and gastropod abundance being 0.010123 and eelgrass coverage and crustacean abundance being 0.008273. These numbers indicated that only a small proportion of the variance in the number of gastropod and crustacean abundance could be explained by the coverage of the eelgrass, which signified that despite the statistical significance shown from the p-value, the relationship between the 2 variables is rather weak. On the other hand, no statistically significant correlation was observed between the eelgrass edge and epifauna, gastropod, and crustacean abundance due to the p-values from the results being ≤ 1 .

| Ratio | | | | Edge | | | |
|-----------------|---------------------|----------|----------|-----------------|---------------------|----------|----------|
| Buffer Size (m) | Epifauna | P-value | R Square | Buffer Size (m) | Epifauna | P-value | R Square |
| 0.5 | Epifana_abundnace | 0.482732 | 0.00122 | 0.5 | Epifana_abundnace | 0.820549 | 0.000128 |
| | crustacea_abundance | 0.178858 | 0.004469 | | crustacea_abundance | 0.88242 | 5.42E-05 |
| | gastropod_abundance | 0.888756 | 4.85E-05 | | gastropod_abundance | 0.886568 | 5.04E-05 |
| 1 | Epifana_abundnace | 0.880873 | 5.57E-05 | 1 | Epifana_abundnace | 0.308471 | 0.002567 |
| | crustacea_abundance | 0.296286 | 0.0027 | | crustacea_abundance | 0.425838 | 0.00157 |
| | gastropod_abundance | 0.288301 | 0.003494 | | gastropod_abundance | 0.642548 | 0.000534 |
| 2 | Epifana_abundnace | 0.912344 | 3.00E-05 | 2 | Epifana_abundnace | 0.37924 | 0.001914 |
| | crustacea_abundance | 0.067126 | 0.008273 | | crustacea_abundance | 0.801516 | 0.000157 |
| | gastropod_abundance | 0.042741 | 0.010123 | | gastropod_abundance | 0.362814 | 0.00205 |

Table 2. Summary of the 18 linear regression tests conducted for the first set of studies, where data from all years are taken into consideration. Cells indicating a statistically significant p-value are highlighted in yellow

Table 3 presents the results of the second set of analyses, which separated the data by the years of 2019 and 2021. The results displayed a generally minimal relationship between eelgrass and the epifauna species. In the regression tests between eelgrass coverage and epifauna/ gastropod/ crustacean abundance, it was noted that the analyses from 2019 for the

0.5 m buffer zone showed surprising results, where p-values of 0.083801 and 0.099705 resulted from the regression testes between eelgrass and epifauna and crustacean abundance, respectively. Despite the statistically significant results for epifauna and crustacean abundance, gastropod abundance has a p-value of 0.403081, where no statistical significance was observed. Similarly, the results from the 2 m buffer zones also indicated a strong correlation between those 2 variables. Moreover, 2021 results highlighted a significant relationship between eelgrass and gastropod abundance in the 2 m buffer, with a p-value of 0.014995. Despite the significant correlation present between eelgrass coverage and some of the biological variables, the correlation between the 2 variables is relatively weak on a scale of 0 - 1. On the other hand, similar to the first set of analyses, the results on the eelgrass edge length side indicated a non-significant relationship as they are mostly in a range of 0.3 - 0.9.

| Ratio | | | | Edge | | | | | | | |
|-----------------|------|---------------------|---------------------|----------|-----------------|---------------------|---------------------|-------------|---------------------|----------|----------|
| Buffer Size (m) | Year | Epifauna | P-value | R Square | Buffer Size (m) | Year | Epifauna | P-value | R Square | | |
| 0.5 | 19 | Epifana_abundnace | 0.083801 | 0.013651 | 0.5 | 19 | Epifana_abundnace | 0.873944 | 0.000116 | | |
| | | crustacea_abundance | 0.099705 | 0.012384 | | | crustacea_abundance | 0.478451 | 0.002307 | | |
| | | gastropod_abundance | 0.403081 | 3.21E-03 | | | gastropod_abundance | 0.390373 | 3.39E-03 | | |
| | 21 | Epifana_abundnace | 0.80251 | 0.000345 | | 21 | Epifana_abundnace | 0.86485 | 0.00016 | | |
| | | crustacea_abundance | 0.582593 | 0.001663 | | | crustacea_abundance | 0.690917 | 0.000871 | | |
| | | gastropod_abundance | 0.502824 | 0.002471 | | | gastropod_abundance | 0.625923 | 0.001308 | | |
| | 1 | 19 | Epifana_abundnace | 0.24552 | | 0.006181 | 1 | 19 | Epifana_abundnace | 0.430324 | 0.002855 |
| | | | crustacea_abundance | 0.20038 | | 0.00751 | | | crustacea_abundance | 0.314684 | 0.004637 |
| | | | gastropod_abundance | 0.731375 | | 0.000542 | | | gastropod_abundance | 0.945817 | 2.12E-05 |
| 21 | | Epifana_abundnace | 0.439527 | 0.003287 | 21 | Epifana_abundnace | | 0.458612 | 0.003022 | | |
| | | crustacea_abundance | 0.549854 | 0.001968 | | crustacea_abundance | | 0.809444968 | 0.00032 | | |
| | | gastropod_abundance | 0.113697 | 0.013691 | | gastropod_abundance | | 0.48553 | 0.002676 | | |
| 2 | | 19 | Epifana_abundnace | 0.0553 | 1.67E-02 | 2 | | 19 | Epifana_abundnace | 0.795001 | 0.00031 |
| | | | crustacea_abundance | 0.017547 | 0.025601 | | | | crustacea_abundance | 0.888786 | 8.99E-05 |
| | | | gastropod_abundance | 0.79885 | 0.000299 | | | | gastropod_abundance | 0.877479 | 0.000109 |
| | 21 | Epifana_abundnace | 0.261556 | 0.006921 | 21 | | Epifana_abundnace | 0.269338 | 0.0067 | | |
| | | crustacea_abundance | 0.400114 | 0.003893 | | | crustacea_abundance | 0.738095 | 0.000616 | | |
| | | gastropod_abundance | 0.014995 | 0.032075 | | | gastropod_abundance | 0.228351 | 0.007963 | | |

Table 3. Summary of the 36 linear regression tests conducted for the second set of studies, where data from the years of 2019 and 2021 are separated. Cells indicating a statistically significant p-value are highlighted in yellow

Discussion and Conclusion

Enhanced Eelgrass Habitat Mapping with Drones

The use of drone technology in this study produced high-resolution imagery for the assessment of eelgrass coverage and eelgrass edge length along coastal regions. The enhanced quality of the orthomosaic enabled detailed analyses, including the classification and

delineation of eelgrass meadows and the digitization of transect lines, on the eelgrass habitats. In terms of obtaining high-quality imagery data, this improved data collection method with drones offered a relatively more cost-efficient and flexible approach compared to traditional commercial satellite data. The advancement of UAV technology has proven crucial for examining various habitat dynamics in the study. Moreover, the ongoing development of remote sensing and classification methods would provide more accurate results for future ecological assessment.

Eelgrass Coverage/Edge Length and Epifauna Abundance

The p-values and R-squared resulted from the linear regression tests provide vital information on the statistical significance and correlation between the dependent and independent variables. From the results, it was noticed that the statistical relationship between eelgrass coverage and epifauna (including gastropods and crustaceans) was generally moderate, and the eelgrass edge length and epifauna abundance showed minimal statistical significance. However, in larger buffer zones (2 m), the results indicated a significant correlation between the 2 variables. This likely suggested that a broader area of eelgrass meadows potentially provided more resources for the surrounding epifauna, which could support a higher abundance of the more mobile species. While the p-value is within the threshold, the low R-squared value might signify that eelgrass was not the sole factor that influenced epifauna abundance. Other environmental and ecological variables might contribute to a stronger and more significant relationship to the epifauna. Potential independent variables such as water quality, temperature, and seabed sediment quality could be incorporated into future studies.

Temporal Variability of Eelgrass and Epifauna Relationships

The second set of statistical analyses incorporated temporal variability in studying how eelgrass characteristics impacted epifauna abundance across different years. Similarly, we noticed a more statistically significant relationship between eelgrass coverage and some epifauna abundance in the 2-m buffer zones, while eelgrass edge length presented statistical

significance. In addition, the results from the 0.5-m buffer zones showed a significant relationship between the 2 variables in 2019 but not in 2021. While it was uncertain on the specific factors that caused this temporal variation, it was presumed that environmental factors such as the eelgrass wasting disease and the warming of sea surface temperatures could play a key role in the change of the eelgrass distribution across years (Graham, et.al.,2023), which potentially led to the results indicated in our studies.

Limitation and Future Studies

It is presumed that several limitations in the study might influence the result of the analyses. For instance, some of the sampling point locations were inferred due to the lack of the exact coordinates of transect points in the 2020 data, which could potentially introduce discrepancies between the epifauna data location and the buffer zones of the eelgrass. In addition, there was missing epifauna data for the years of 2020 and 2021 in certain sites due to COVID-19, which potentially led to a smaller and less representative sample size. Moreover, the lack of statistical significance in the relationship between eelgrass edge length and epifauna abundance could have originated from the manual digitization of the eelgrass from the transect tape-filling process. The inferred location of the eelgrass at transect tapes might have introduced errors when calculating the eelgrass edge length. Since the eelgrass classification process conducted in eCognition was a supervised classification method, there was a significant challenge when distinguishing eelgrass from similar-looking aquatic vegetations like algae due to their similar color. Eelgrass could sometimes be indistinguishable from algae in drone images, which could potentially lead to misclassification and inaccuracies in the training data. To address these limitations in future studies, improvements could be made to the data selection process to only analyze the sample points that locations are certain of. Moreover, increasing the number of sampling points for the eelgrass coverage and epifauna data could help create more represented data. Last but not least, revisions of the parameters set in the segmentation process would allow the better delineation of the eelgrass segments, which might further

enhance the accuracy of the sample selections and classification. Refining these aspects could mitigate limitations and improve the overall reliability and precision of the analyses. This larger-scale study covering the entire Northeast Pacific coast provides a comprehensive view of the variations in eelgrass coverage and epifauna abundance. To better understand and address these regional differences, future studies could explore the use of different statistical methods like linear mixed model.

In conclusion, our research has proven drone-assisted mapping to be a transformative tool for coastal ecology studies. The framework developed in this study provides insights into the conservation and management of eelgrass habitats and epifauna diversity. We hope that as drone and remote sensing technologies continue to mature and evolve, more innovative coastal management strategies can be established and implemented.

Bibliography

- Andriolo, U., Gonçalves, G., Sobral, P., & Bessa, F. (2021). Spatial and size distribution of macro-litter on coastal dunes from drone images: A case study on the Atlantic coast. *Marine Pollution Bulletin*, 169, 112490. <https://doi.org/10.1016/j.marpolbul.2021.112490>
- Adade, R., Aibinu, A. M., Ekumah, B., & Asaana, J. (2021). Unmanned Aerial Vehicle (UAV) Applications in coastal zone management—a review. *Environmental Monitoring and Assessment*, 193(3). <https://doi.org/10.1007/s10661-021-08949-8>
- Briones-Fourzán, P., Monroy-Velázquez, L. V., Estrada-Olivo, J., & Lozano-Álvarez, E. (2020). Diversity of seagrass-associated decapod crustaceans in a tropical reef lagoon prior to large environmental changes: A baseline study. *Diversity*, 12(5), 205. <https://doi.org/10.3390/d12050205>
- Boström, C., Baden, S., Bockelmann, A., Dromph, K., Fredriksen, S., Gustafsson, C., Krause-Jensen, D., Möller, T., Nielsen, S. L., Olesen, B., Olsen, J., Pihl, L., & Rinde, E. (2014). Distribution, structure and function of Nordic eelgrass (*Zostera marina*) ecosystems: Implications for coastal management and conservation. *Aquatic Conservation: Marine and Freshwater Ecosystems*, 24(3), 410–434. <https://doi.org/10.1002/aqc.2424>
- Colomina, I., & Molina, P. (2014). Unmanned aerial systems for photogrammetry and Remote Sensing: A Review. *ISPRS Journal of Photogrammetry and Remote Sensing*, 92, 79–97. <https://doi.org/10.1016/j.isprsjprs.2014.02.013>
- Coffer, M. M., Schaeffer, B. A., Zimmerman, R. C., Hill, V., Li, J., Islam, K. A., & Whitman, P. J. (2020). Performance across worldview-2 and RapidEye for reproducible seagrass mapping. *Remote Sensing of Environment*, 250, 112036. <https://doi.org/10.1016/j.rse.2020.112036>
- Duffy, J. E., Benedetti-Cecchi, L., Trinanes, J., Muller-Karger, F. E., Ambo-Rappe, R., Boström, C., Buschmann, A. H., Byrnes, J., Coles, R. G., Creed, J., Cullen-Unsworth, L. C., Diaz-Pulido, G., Duarte, C. M., Edgar, G. J., Fortes, M., Goni, G., Hu, C., Huang, X., Hurd, C. L., ... Yaakub, S. M. (2019). Toward a coordinated global observing system for seagrasses and marine macroalgae. *Frontiers in Marine Science*, 6. <https://doi.org/10.3389/fmars.2019.00317>
- Ferretto, G., Vergés, A., Poore, A. G., Glasby, T. M., & Griffin, K. J. (2023). Habitat provision and erosion are influenced by seagrass meadow complexity: A seascape perspective. *Diversity*, 15(2), 125. <https://doi.org/10.3390/d15020125>
- Favaro, Brett; Zargarpour, Nicola (2018). Using unmanned aerial vehicles for the study of eelgrass habitat. figshare. Journal contribution. <https://doi.org/10.6084/m9.figshare.6210608.v1>
- Graham, O. J., Stephens, T., Rappazzo, B., Klohmann, C., Dayal, S., Adamczyk, E. M., Olson, A., Hessing-Lewis, M., Eisenlord, M., Yang, B., Burge, C., Gomes, C. P., & Harvell, D. (2023). Deeper habitats and cooler temperatures moderate a climate-driven seagrass disease. *Philosophical Transactions of the Royal Society B: Biological Sciences*, 378(1873). <https://doi.org/10.1098/rstb.2022.0016>
- Hily, C., Connan, S., Raffin, C., & Wyllie-Echeverria, S. (2004). In vitro experimental assessment of the grazing pressure of two gastropods on *Zostera marina* L. epiphytic algae. *Aquatic Botany*, 78(2), 183–195. <https://doi.org/10.1016/j.aquabot.2003.10.001>

- Klemas, V. V. (2015). Coastal and environmental remote sensing from unmanned aerial vehicles: An overview. *Journal of Coastal Research*, 315, 1260–1267.
<https://doi.org/10.2112/jcoastres-d-15-00005.1>
- Kandrot, S., Hayes, S., & Holloway, P. (2021). Applications of uncrewed aerial vehicles (UAV) technology to support Integrated Coastal Zone Management and the UN Sustainable Development Goals at the Coast. *Estuaries and Coasts*, 45(5), 1230–1249.
<https://doi.org/10.1007/s12237-021-01001-5>
- Marin Jarrin, M. J., Sutherland, D. A., & Helms, A. R. (2022). Water temperature variability in the coos estuary and its potential link to eelgrass loss. *Frontiers in Marine Science*, 9.
<https://doi.org/10.3389/fmars.2022.930440>
- Plaisted, H. K., Shields, E. C., Novak, A. B., Peck, C. P., Schenck, F., Carr, J., Duffy, P. A., Evans, N. T., Fox, S. E., Heck, S. M., Hudson, R., Mattera, T., Moore, K. A., Neikirk, B., Parrish, D. B., Peterson, B. J., Short, F. T., & Tinoco, A. I. (2022). Influence of rising water temperature on the temperate Seagrass Species Eelgrass (*zostera marina* L.) in the northeast USA. *Frontiers in Marine Science*, 9. <https://doi.org/10.3389/fmars.2022.920699>
- Román, A., Tovar-Sánchez, A., Olivé, I., & Navarro, G. (2021). Using a UAV-mounted multispectral camera for the monitoring of marine macrophytes. *Frontiers in Marine Science*, 8. <https://doi.org/10.3389/fmars.2021.722698>
- Tak, W. J., Jun, K. W., Kim, S. D., & Lee, H. J. (2020). Using drone and Lidar to assess coastal erosion and shoreline change due to the construction of coastal structures. *Journal of Coastal Research*, 95(sp1), 674. <https://doi.org/10.2112/si95-131.1>
- Taylor, R. B. (2019). Epiflora and Epifauna. *Encyclopedia of Ecology*, 375–380.
<https://doi.org/10.1016/b978-0-12-409548-9.10922-4>
- Tahara, S., Sudo, K., Yamakita, T., & Nakaoka, M. (2022). Species level mapping of a seagrass bed using an unmanned aerial vehicle and deep learning technique. *PeerJ*, 10.
<https://doi.org/10.7717/peerj.14017>
- TRUEMAN, E. R. (1983). Locomotion in molluscs. *The Mollusca*, 155–198.
<https://doi.org/10.1016/b978-0-12-751404-8.50012-8>
- Whippo, R., Knight, N. S., Prentice, C., Cristiani, J., Siegle, M. R., & O'Connor, M. I. (2018). Epifaunal diversity patterns within and among seagrass meadows suggest landscape-scale biodiversity processes. *Ecosphere*, 9(11). <https://doi.org/10.1002/ecs2.2490>
- Ward, D. H., Hogrefe, K. R., Donnelly, T. F., Fairchild, L. L., Sowl, K. M., & Lindstrom, S. C. (2022). Abundance and distribution of eelgrass (*zostera marina*) and seaweeds at Izembek National Wildlife Refuge, Alaska, 2007–10. Open-File Report.
<https://doi.org/10.3133/ofr20201035>
- Yang, B., Hawthorne, T. L., Torres, H., & Feinman, M. (2019). Using object-oriented classification for coastal management in the East Central Coast of Florida: A quantitative comparison between UAV, satellite, and Aerial Data. *Drones*, 3(3), 60.
<https://doi.org/10.3390/drones3030060>
- Yang, B., Hawthorne, T. L., Hessing-Lewis, M., Duffy, E. J., Reshitnyk, L. Y., Feinman, M., & Searson, H. (2020). Developing an introductory UAV/drone mapping training program for Seagrass Monitoring and Research. *Drones*, 4(4), 70.
<https://doi.org/10.3390/drones4040070>

Yang, B., Hawthorne, T. L., Aoki, L., Beatty, D. S., Copeland, T., Domke, L. K., Eckert, G. L., Gomes, C. P., Graham, O. J., Harvell, C. D., Hovel, K. A., Hessing-Lewis, M., Harper, L., Mueller, R. S., Rappazzo, B., Reshitnyk, L., Stachowicz, J. J., Tomas, F., & Duffy, J. E. (2023). Low-altitude UAV imaging accurately quantifies eelgrass wasting disease from Alaska to California. *Geophysical Research Letters*, 50(4).
<https://doi.org/10.1029/2022gl101985>